RIGA TECHNICAL UNIVERSITY

Anish Niranjan Kulkarni

MICRO-DAMAGE EVOLUTION IN NOVEL POLYMER COMPOSITE MATERIALS

Summary of the Doctoral Thesis

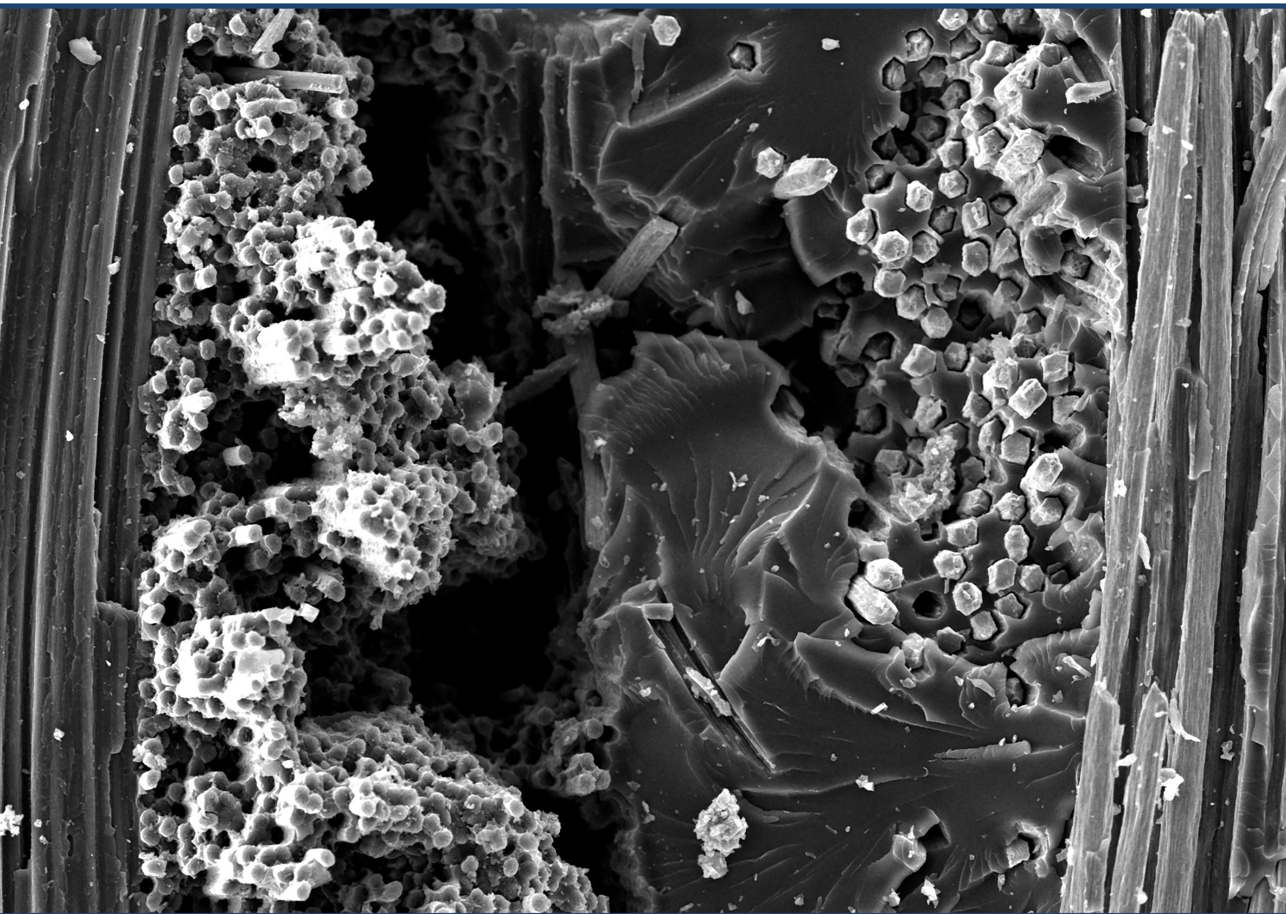

RTU Press
Riga 2026

RIGA TECHNICAL UNIVERSITY

Faculty of Civil and Mechanical Engineering

Institute of High-Performance Materials and Structures

Anish Niranjan Kulkarni

Doctoral Student of the Study Programme "Mechanical Engineering and Mechanics (Applied Mechanics)"

MICRO-DAMAGE EVOLUTION IN NOVEL POLYMER COMPOSITE MATERIALS

Summary of the Doctoral Thesis

Scientific supervisor
Professor Dr. sc. ing.
ANDREJS PUPURS

RTU Press
Riga 2026

Kulkarni, A. N. Micro-Damage Evolution in Novel Polymer Composite Materials. Summary of the Doctoral Thesis. Riga: RTU Press, 2026. 40 p.

Published in accordance with the decision of the Promotion Council "RTU P-04" of March 30th, 2026, Minutes No. 04030-9.4/7.

Cover image by Anish Niranjan Kulkarni.

https://doi.org/10.7250/9789934373374
ISBN 978-9934-37-337-4 (pdf)

ACKNOWLEDGEMENTS

The Doctoral Thesis research was supported by the following funding resources:

- European Social Fund within the Project No. 8.2.2.0/20/I/008 "Strengthening of PhD students and academic personnel of Riga Technical University and BA School of Business and Finance in the strategic fields of specialization" of the Specific Objective 8.2.2 "To Strengthen Academic Staff of Higher Education Institutions in Strategic Specialization Areas" of the Operational Programme "Growth and Employment".
- Doctoral grant (No. 1061) under Project No. 5.2.1.1.i.0/2/24/I/CFLA/003 – Implementation of consolidation and management changes at Riga Technical University, LiepU, RTA, LJA and LJK towards excellence in higher education, science and innovation.
- Latvian Council of Science, Fundamental and Applied Research Project No. LZP-2019/1-0357: *Development and behavior analysis of novel textile composite/metal joints with enhanced mechanical properties* [TXJOIN].
- Latvian Council of Science, Fundamental and Applied Research Project No. LZP-2022/1-0572: *Development of innovative induction-heating system for manufacturing of high-performance composites with improved mechanical properties* [DINCIP].
- State Research Programme "Sports" Project No. VPP-IZM-Sports-2023/1-0001: Innovations, methodologies and recommendations for the development and management of the sports sector in Latvia [VPP SPORTS/IMRSportsLV].
- European Union Recovery and Resilience Facility funded Project No. 5.2.1.1.i.0/2/24/I/CFLA/003 "Implementation of consolidation and management changes at RTU, LiepU, Rēzekne Academy of Technology and Latvian Maritime Academy and Liepāja Maritime College for progress towards excellence in higher education, science and innovation". Scientist grant project No. RTU-ZG-2024/1-0013.

PREFACE

I cannot begin without saying a huge thanks to Andrejs, Līva and Jānis for being the best advisors, guardians, mentors and friends that I could ever have. Thanks for making me part of the family (or families, be it the Pupurs, IHPMS, BMF, LTU, …), and for introducing me to potatoes and dill – they do go well together (sometimes :).

The Thesis is dedicated to Aai and Baba, who have supported me tirelessly throughout this journey. This was a hard grind; and being homesick was but natural. Thanks to them for always being there, for believing in my dreams, for cheering me up when I was down, and for making sure that I sail through to the other side.

Moving to Riga was not the easiest decision for me, but this city has given me so much over the four years. It has given me my best buddies, Vivek and Farshad, without whom I simply cannot imagine my time here. We had the best of times, and it was a pleasure to challenge you both several times at our friendly games of table tennis.

Of course, thanks to the Maharashtrians in Riga – Akshay, Raveena, Avaneesh, Bhavesh, Anfal, Vilol, Trupti and Prafulla. Wouldn't have imagined celebrating Ganeshotsav, Diwali, and eating Misal in Riga without you guys.

A huge thanks to Kate and Liliana for offering me the best place to stay. Thanks for being the sweetest homeowners. I owe a lot to Mastu 3, and to both of you.

Then there's the lunch group at the university, and I am proud to be a founder of this group, along with Renārs, Marina, Andrejs and Jānis. BT1 fed me for four years, and you guys made me go there.

Of course, with Renārs, Līva, Marina, Mārtiņš, Viesturs, Ilgar, Karuna, Ishara, Deivis, Elvijs, Eduards, Lorenzo, Robert, Rihards, Rūdolfs and Jānis it was much more than just the lunch group. It just takes a few co-authors to write a research paper, but it takes a bunch of you guys to survive four years at the most flamboyant and happening place such as a university.

Coming back to the most important person in this journey, thanks, Andrejs, for believing in me. Hopefully one day, I'll be as good a person as you are. Thanks for everything.

Anish Niranjan Kulkarni
Riga, 06.03.2026

DOCTORAL THESIS PROPOSED TO RIGA TECHNICAL UNIVERSITY FOR PROMOTION TO THE SCIENTIFIC DEGREE OF DOCTOR OF SCIENCE

To be granted the scientific degree of Doctor of Science (PhD), the present Doctoral Thesis has been submitted for defence at the open meeting of the RTU Promotion Council on 9 October 2026, at 10:00, at the Faculty of Civil and Mechanical Engineering of Riga Technical University, Ķīpsalas iela 6A, auditorium 135.

OFFICIAL REVIEWERS

Professor Martin Fagerström
Chalmers University of Technology, Sweden

Professor Endel Iarve
The University of Texas at Arlington, USA

Dr. phys. Sergejs Tarasovs
University of Latvia, Latvia

DECLARATION OF ACADEMIC INTEGRITY

I hereby declare that the Doctoral Thesis submitted for review to Riga Technical University for promotion to the scientific degree of Doctor of Science (PhD) is my own. I confirm that this Doctoral Thesis has not been submitted to any other university for promotion to a scientific degree.

Anish Niranjan Kulkarni ……………………………. (signature)
Date: …………………………….

The Doctoral Thesis has been written in English as a collection of six scientific publications. It consists of a summary of 40 pages, including 20 figures, two tables, and 54 titles in the bibliography. The summary contains an introduction to the Thesis topic, the main results of the Thesis, and six appended papers. The papers are written in English, and their total length is 90 pages.

CONTENTS

ABBREVIATIONS AND SYMBOLS

FEM	finite element method
CF	carbon fiber
UD	unidirectional
ERR	energy release rate
GF/EP	glass-fiber/epoxy composite
CF/EP	carbon-fiber/epoxy composite
ρ	transverse crack density
ρ_n	normalized crack density
σ_T	transverse stress
σ_{Tn}	normalized transverse stress
d	half-thickness of 90-layer in [0,90]s cross-ply laminate (Section 2.1)
t_0	thickness of 0-layer in [0,90]s cross-ply laminate
t_{90}	thickness of 90-layer in [0,90]s cross-ply laminate
G	energy release rate
G_T	total energy release rate
a_N	transverse crack length (Section 2.1)
E_L^0	longitudinal elastic modulus of 0-layer in [0,90]s cross-ply laminate
G_{LT}^0	in-plane shear modulus of 0-layer in [0,90]s cross-ply laminate
E_T^{90}	transverse elastic modulus of 90-layer in [0,90]s cross-ply laminate
l_d	delamination length (Section 2.1)
l_c	half-distance between two adjacent transverse cracks (Section 2.1)
E_{x0}	initial longitudinal elastic modulus of composite (Section 2.2)
ROM	rule of mixtures
SEM	scanning electron microscopy
RVE	representative volume element
3D	three-dimensional
D_L	longitudinal damage parameter of composite RVE (Section 2.2)
X_T	longitudinal tensile strength of composite RVE (Section 2.2)
Y_T	transverse tensile strength of composite RVE (Section 2.2)
S_L	longitudinal shear strength of composite RVE (Section 2.2)
DSC	differential scanning calorimetry
T_g	glass transition temperature
E	elastic modulus of composite (Section 2.3)

E_n	normalized elastic modulus of composite (Section 2.3)
$\sigma_{\max}$	ultimate tensile strength of composite (Section 2.3)
$\varepsilon_{\max}$	strain-to-failure of composite (Section 2.3)

GENERAL OVERVIEW OF THE THESIS

The Doctoral Thesis unites six thematically connected publications. The main objective of the doctoral thesis is to study the micro-damage evolution in polymer composite materials with i) high crack density, ii) novel hybrid textile meso-structure, and iii) novel manufacturing method of electromagnetic induction heating.

Paper I and **Paper II** address the micro-damage in the form of transverse (intralaminar) cracks and interlaminar delamination cracks in [0,90]s cross-ply laminates. Under uniaxial quasi-static tensile loading, the propagation of transverse cracks and delaminations has been numerically studied using FEM by analyzing changes in the strain energy release rate available for crack growth. The novelty of this study lies in i) analyzing growth of a new transverse crack growing in the regions of high crack density with prominent transverse stress gradients along the 90-ply thickness direction, and ii) conducting a detailed analysis of parameters (including geometrical parameters, material constants and transverse crack density) responsible for the symmetrical or non-symmetrical growth of local delaminations initiated at the tips of transverse cracks.

Papers III, **IV,** and **V** address the initiation and propagation of micro-damage in hybrid carbon/steel fiber textile composites. The hybrid composites are manufactured with plain woven or plain weft knitted fabric reinforcement and an epoxy matrix. Under uniaxial quasi-static tensile loading along the warp yarn direction, these composite laminates exhibit micro-damage in the form of weft yarn/matrix-interface delaminations and fiber breaks in the warp yarns. The numerical study of the mechanical behavior of hybrid carbon/steel fiber textile composites using FEM shows that the fiber breaks in the carbon fiber warp yarns strongly affect the composite's macro-mechanical behavior. The novelty of this study lies in the manufacturing of hybrid carbon/steel fiber textile composites and the application of the elastoplastic damage model developed by Cózar et al. [1], [2] to simulate the mechanical behavior of the hybrid textile composite materials.

Paper VI addresses micro-damage evolution in carbon fiber (CF)-reinforced thermoset composites manufactured using an electromagnetic induction heating system with a moving-coil design. Induction heating of a CF-reinforced thermoset composite with a stationary coil results in the formation of a cold spot. Although a moving-coil design mitigates the formation of a single cold spot, it creates a time-varying temperature gradient in the composite, leading to the entrapment of air bubbles formed during curing. Thus, large void content can be observed in the induction-cured composites that affects the initiation of micro-damage under mechanical loading. The novelty of this study lies in the manufacturing of induction-cured CF-reinforced thermoset composites and the comparison of the mechanical behavior of induction-cured and oven-cured reference composites under uniaxial quasi-static tensile loading.

Objective and tasks

The main objective of the Thesis is to study the evolution of micro-damage mechanisms such as transverse cracks and delaminations in composite materials with:

i) a damage state not studied in the literature, i.e., high crack density;

ii) a novel meso-structure, i.e., hybrid carbon/steel fiber textile meso-structure;

iii) a novel electromagnetic induction heating manufacturing process.

Scientific novelty and main results

The scientific novelty of the Thesis lies in the study of micro-damage mechanisms in i) polymer composites with high crack density; ii) hybrid carbon/steel fiber composites with textile meso-structure; and iii) polymer composites manufactured by means of electromagnetic induction heating. The main results obtained in the Thesis are as follows.

1. In the high crack density regions in 90-layers in cross-ply laminates under uniaxial tensile loading, high gradients in transverse stress are generated along the thickness direction. Such gradients in stress strongly affect the strain energy release rate available for the growth of a new transverse crack.
2. Due to high stress concentrations at the transverse crack tips, local delaminations are generated in cross-ply laminates under uniaxial tensile loading. The delaminations grow symmetrically or non-symmetrically with respect to the existing transverse crack and the laminate midplane, forming I-shaped, T-shaped, C-shaped, or S-shaped cracks. The growth of these delaminations depends on the transverse crack density, 0/90-layer thickness ratio, and 0/90-layer stiffness ratios. A non-symmetrical I-shaped delamination tends to grow into a symmetrical I-shaped delamination before growing further.
3. In hybrid carbon/steel fiber woven composites under uniaxial quasi-static tensile loading along the warp yarn direction, micro-damage initiates in the form of weft yarn/matrix-interface delaminations. Upon further loading, fiber breaks are observed in the warp yarns that strongly affect the composite’s macro-mechanical behavior. A cluster of fiber breaks results in warp yarn failure and is accompanied by the ultimate failure of the hybrid composite.
4. During the manufacturing of carbon fiber-reinforced epoxy composites using electromagnetic induction heating, a moving-coil design mitigates the problem of the formation of a cold spot. But it allows the entrapment of air bubbles generated during curing due to a time-varying temperature gradient in the composite material. This results in a large void content in the induction-cured composite specimens. Under uniaxial tensile loading, the voids help in the micro-damage initiation in induction-cured composites at a lower applied strain level than the oven-cured reference composites.

Structure of the Thesis

The summary of the Doctoral Thesis contains the introduction to the Thesis topic and the main results of the Thesis. The chapter on the main results has three sections: Micro-damage evolution in cross-ply laminates with high crack density, Micro-damage evolution in hybrid carbon/steel fiber textile composites, and Micro-damage evolution in induction-cured thermoset composites. It also contains six appended publications, which are listed in the Section "Publications and approbation of the Thesis".

The Doctoral Thesis has been written in English. It consists of a summary of 40 pages, including 20 figures, two tables, and 54 titles in the bibliography. The summary contains an introduction to the thesis topic, the main results of the Thesis, and six appended publications. The publications are written in English, and their total length is 90 pages.

Publications and approbation of the Thesis

Paper I

Kulkarni AN, Pupurs A, Varna J. Analysis of initiation and growth of new transverse cracks in high crack density regions in cross-ply laminates. J Compos Mater 2025; 59: 539–50. https://doi.org/10.1177/00219983241295811.

Paper II

Kulkarni AN, Pupurs A, Varna J. Parameters affecting growth of local delaminations at transverse crack tips in [0m,90n]s cross-ply laminates. Eng Fract Mech 2025; 328: 111549. https://doi.org/10.1016/J.ENGFRACMECH.2025.111549.

Paper III

Kulkarni AN, Pupurs A, Šņepsts A, Irbe M. MICRO-DAMAGE EVOLUTION IN HYBRID CARBON/STEEL KNITTED AND WOVEN FABRIC COMPOSITES. In: Falzon B, McCarthy C, editors. Proceedings of the 2023 International Conference on Composite Materials, Belfast: Queen's University Belfast; 2023.

Paper IV

Kulkarni AN, Kononova O, Jevstigņejevs V, Pupurs A. FE MODELING OF DAMAGE DEVELOPMENT IN HYBRID CARBON/STEEL FIBER TEXTILE COMPOSITES USING FRACTURE MECHANICS AND COHESIVE ZONE APPROACH. In: Binetruy C, Jacquemin F, editors. Proceedings of the 21st European Conference on Composite Materials, Nantes: The European Society for Composite Materials (ESCM) and the Ecole Centrale de Nantes; 2024, pp. 1362–68.

Paper V

Kulkarni AN, Pupurs A, Kononova O, Jevstigņejevs V, Maimi P, Subramani A. Parametric study of micro-damage evolution in woven hybrid carbon/stainless steel fiber composites. In preparation.

Paper VI

Pupurs A, Lācis V, Šņepsts A, **Kulkarni AN**, Irbe M. ANALYSIS OF MICRO-DAMAGE EVOLUTION IN INDUCTION-CURED THERMOSET COMPOSITES. In: Binetruy C, Jacquemin F, editors. Proceedings of the 21st European Conference on Composite Materials, Nantes: The European Society for Composite Materials (ESCM) and the Ecole Centrale de Nantes; 2024, pp. 1529–34.

Results of the Thesis were presented at the following international conferences

1. 20th European Conference on Composite Materials (ECCM20), June 26–30, 2022, Lausanne, Switzerland.
2. 63rd International Scientific Conference of Riga Technical University, Section "Engineering, Mechanics and Mechanical Engineering", October 13, 2022, Riga, Latvia.
3. 81st International Scientific Conference of the University of Latvia, Section "Advanced Composite and Applications", February 16, 2023, Riga, Latvia.
4. 23rd International Conference on Composite Materials (ICCM23), July 31 – August 4, 2023, Belfast, UK.
5. 64th International Scientific Conference of Riga Technical University, Section "Engineering, Mechanics and Mechanical Engineering", October 11, 2023, Riga, Latvia.
6. 82nd International Scientific Conference of the University of Latvia, Section "Advanced Composite and Applications", February 13, 2024, Riga, Latvia.
7. 19th European Mechanics of Materials Conference (EMMC19), May 29–31, 2024, Madrid, Spain.
8. 21st European Conference on Composite Materials (ECCM21), July 2–5, 2024, Nantes, France.
9. TexComp-15 Conference, September 11–13, 2024, Leuven, Belgium.
10. 65th International Scientific Conference of Riga Technical University, Section "Civil and Mechanical Engineering", October 17, 2024, Riga, Latvia.
11. 83rd International Scientific Conference of the University of Latvia, Section "Advanced Composite and Applications", February 11, 2025, Riga, Latvia.
12. 12th International Conference on Composite Testing and Model Identification (CompTest 2025), May 21–23, 2025, Riga, Latvia.
13. 24th International Conference on Composite Materials (ICCM24), August 4–8, 2025, Baltimore, USA.
14. 66th International Scientific Conference of Riga Technical University, Section "Civil and Mechanical Engineering", October 16, 2025, Riga, Latvia.

1. INTRODUCTION

Polymer composite materials consist of a thermosetting or thermoplastic polymer matrix combined with reinforcements such as short discontinuous or long continuous fibers. The fibers can be randomly dispersed in the matrix or aligned in a specific meso-structure. In a fiber-reinforced composite material, fibers act as the primary load-bearing component. Thus, the alignment of fibers with respect to the loading direction is critical in governing the mechanical performance of a composite material. In addition to their lower density compared to metallic materials, polymer composites are well known for providing exceptional stiffness and strength, making them highly suitable for lightweight applications. Today, the use of polymer composite materials has widened in various engineering sectors such as transport (aircraft fuselages and wings, aero-turbine blades, helicopter wings, high-speed trains, military vehicles), energy (wind turbines, hydrogen storage tanks, solar power systems), and infrastructure (pipes, bridges, roofs), as shown in Fig. 1.1.

In the case of composite materials with long fiber reinforcement, the fibers can be i) randomly distributed; ii) aligned parallel to each other, i.e., unidirectional (UD) reinforcement; or iii) in the form of a textile fabric, with warp and weft yarns. Note that in a woven fabric, the warp yarns are placed lengthwise, whereas the weft or fill yarns are later run through the warp yarns widthwise (see Fig. 1.2). According to the service requirements, the individual composite plies can be aligned in different orientations and stacked in a laminate with a specific layup. For example, in **Papers I, II and VI**, a composite laminate with a cross-ply layup is considered, where UD plies are either stacked along the loading direction (0° ply, or 0-ply) or perpendicular to it (90° ply, or 90-ply). Upon uniaxial tensile loading, damage initiates in the 90-plies in cross-ply laminates in the form of transversal debonds at the fiber/matrix-interface [3].

In the composite plies with fibers oriented perpendicular to the loading direction, the damage initiation takes place due to stress concentration at the fiber/matrix interface [4]. The stress concentration arises from the difference in transverse stiffness between the fiber and the matrix. A localized fiber-matrix debond is created, and upon increase in loading, the adjacent debonds coalesce to form a matrix crack (see Fig. 1.3). With a further increase in loading, in the case of a cross-ply laminate, the matrix crack in the 90-layer grows along the ply thickness direction as a "transverse crack" until it reaches the stiffer 0-layer [5], [6]. In the commonly used analytical models studying the stress state in damaged 90-plies, it is assumed that a transverse crack grows instantaneously along the fiber direction (i.e., along the laminate width direction) until a free surface is reached, creating a tunnelling crack [7]–[11]. This assumption may not be valid for laminates with thin plies, where transverse cracking gets partially or totally suppressed [5].

In textile composites loaded along the warp yarn direction, micro-damage initiates as a fiber/matrix-interface debond at the weft yarn/matrix boundary. The coalescence of debonds takes place either to form a transverse crack inside the weft yarn or a delamination at the weft yarn/matrix-interface [12]. Figure 1.4 shows examples of i) a transverse crack in [0,90]s cross-ply laminate, ii) a weft yarn/matrix-delamination, and iii) a transverse crack inside a weft yarn in a textile composite laminate with plain woven meso-structure. The damage evolution in the textile composites takes place in the form of coalescence of yarn/matrix-interface delaminations and transverse cracks as shown in Fig. 1.5 [13], [14].

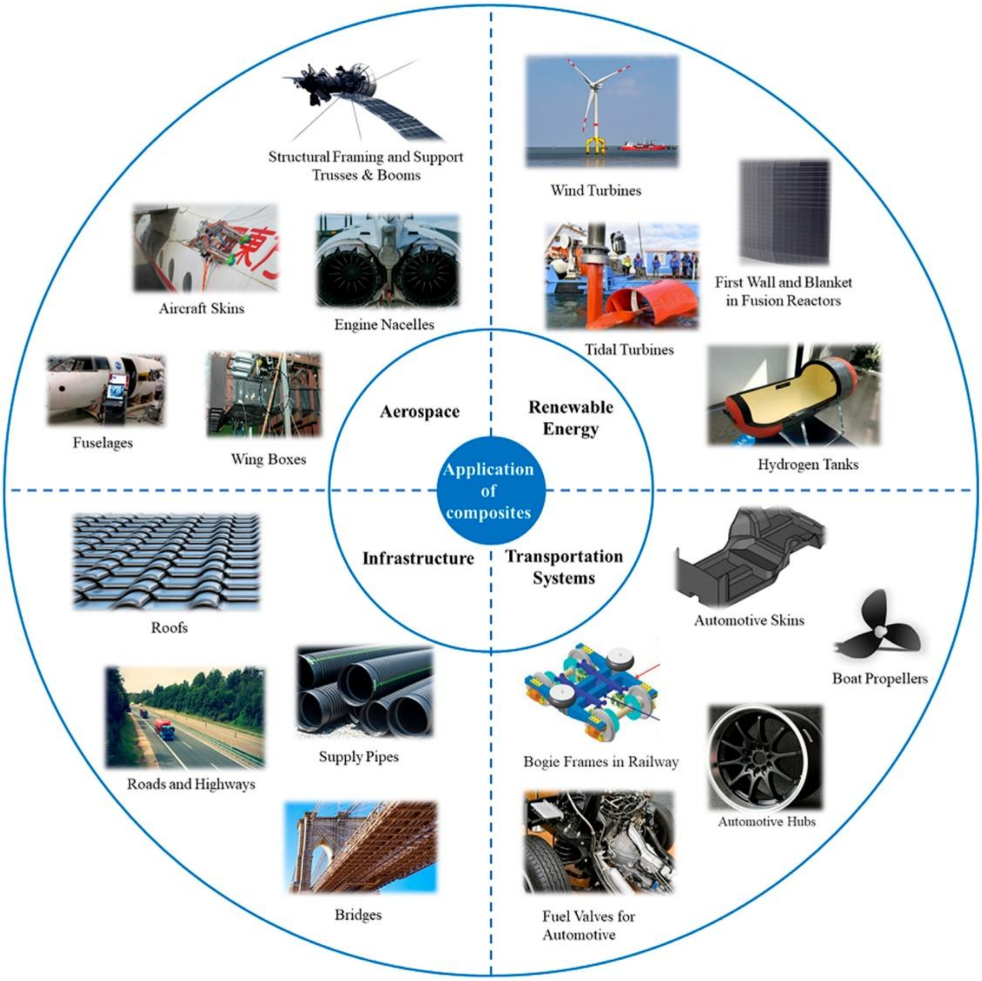

Fig. 1.1. Applications of polymeric composite materials. Reproduced with permission from the publisher and the corresponding author of [15].

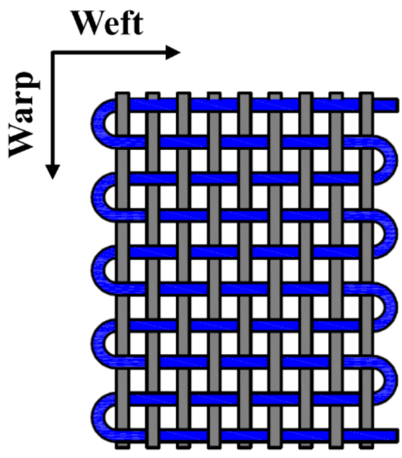

Fig. 1.2. A plain woven textile fabric with warp and weft yarns.

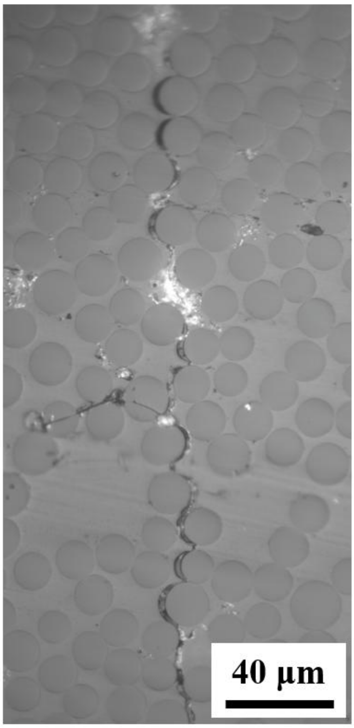

Fig. 1.3. Coalescence of transversal fiber-matrix debonds to form a matrix crack in glass-fiber/epoxy composite laminate [16].

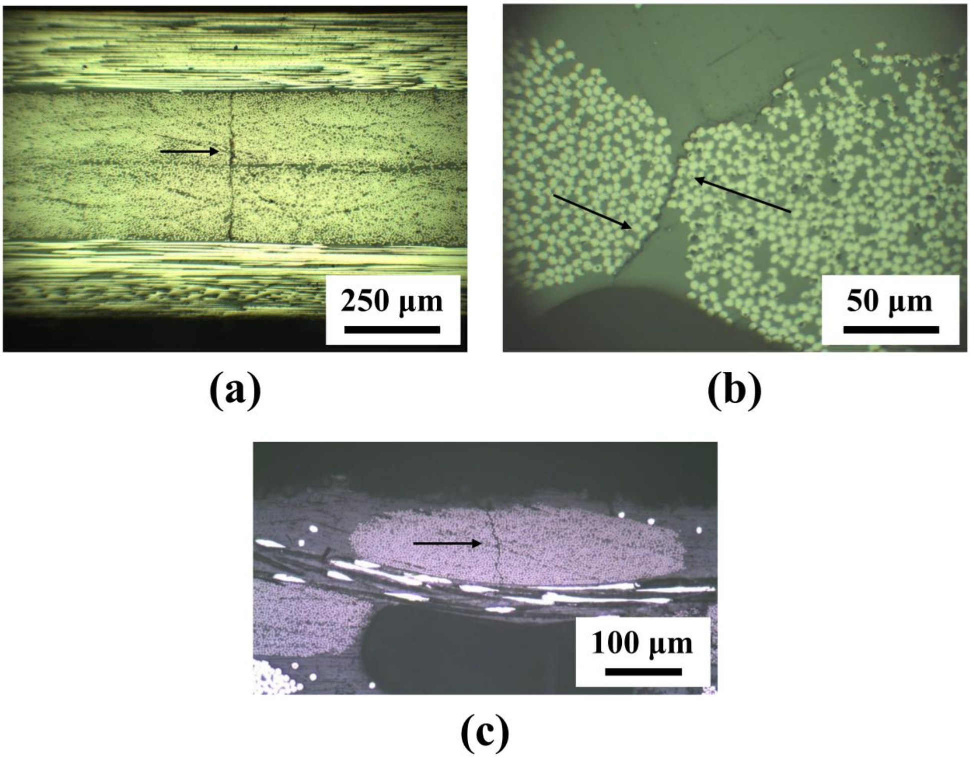

Fig. 1.4. Examples of matrix cracks in carbon-fiber/epoxy composite laminates under uniaxial tensile loading: (a) transverse crack in [0,90]s cross-ply laminate, (b) weft-yarn/matrix delamination, and (c) transverse crack inside a weft yarn in plane woven composite laminate.

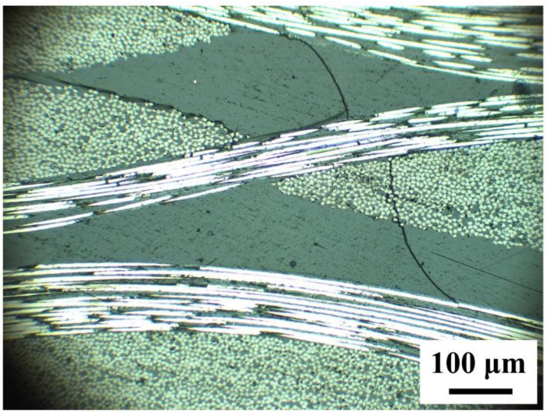

Fig. 1.5. Coalescence of yarn/matrix-interface delaminations and transverse cracks in carbon-fiber/epoxy plane woven composite laminates under uniaxial tensile loading.

In a cross-ply laminate with a transverse crack in the 90-layer, the damaged 90-layer does not carry any load at the location of the transverse crack. At some distance away from the transverse crack, load is transferred back to the 90-layer with the help of out-of-plane shear [11]. Upon further loading, multiple transverse cracking takes place in the 90-layer, increasing the transverse crack density [17]. As the crack density exceeds a threshold, adjacent transverse cracks begin to interact, creating stress perturbations. This reduces the available strain energy release rate (ERR) for the growth of a new transverse crack [18]. Eventually, the transverse crack density reaches saturation [17], [19].

At the transverse crack tip, the generation of very high stresses along the transverse and out-of-plane shear directions causes the formation of a new damage mode, i.e., a local delamination at the tip of an existing transverse crack [6], [20]–[22]. The initiated delamination propagates along the 0/90-layer interface, and it also reduces the available ERR for the growth of a new transverse crack in its vicinity [18]. The growth of a local delamination depends on various parameters, such as 0/90-layer thickness ratio, 0/90-layer stiffness ratios, and transverse crack density [23]. Based on the local stress state, local delaminations can grow into various shapes, such as I-shaped, T-shaped, S-shaped, and C-shaped cracks. Figure 1.6 shows examples of I-shaped and S-shaped delamination cracks in [0,90]s cross-ply laminates.

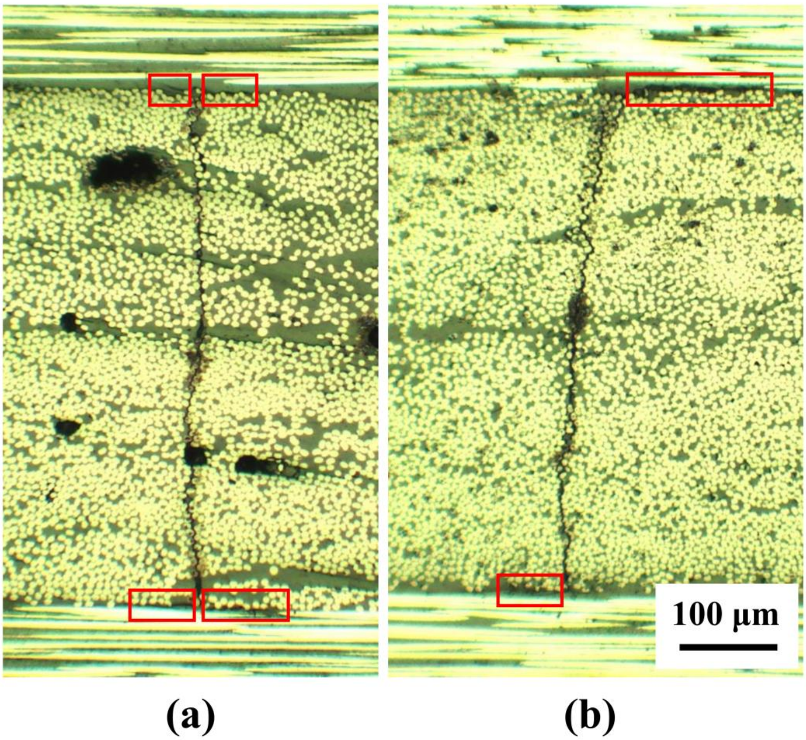

Fig. 1.6. Examples of (a) I-shaped and (b) S-shaped delamination cracks (shown using red rectangles) in carbon-fiber/epoxy [0,90]s cross-ply laminates under uniaxial tensile loading.

The ultimate failure of a thermoset composite laminate often occurs in the form of fiber breakage in the loading direction, catastrophically and in a brittle manner [24]. But some composites can exhibit considerable plasticity before final failure, depending on the specific damage evolution behavior. Epoxy-based composites with ductile steel fiber UD reinforcement exhibit significant plastic behavior under uniaxial tensile loading. They can reach failure strains up to 7 %, which can be further increased using a matrix with higher ductility [25], [26]. UD glass-fiber/epoxy composites hybridized with thin carbon-fiber/epoxy plies can also exhibit “pseudo-ductility” through distributed thin-ply cracking and controlled delamination propagation [27].

In addition to improving ductility and toughness, fiber hybridization can enhance the sustainability of thermoset composites. There are numerous examples of successful industrial applications where glass-fiber/epoxy or carbon-fiber/epoxy composite parts have been hybridized with natural fibers such as flax fibers without a significant loss of the necessary mechanical performance [28]. Recently, there has been an increased interest in some more ‘green’ initiatives in the field of thermoset composites, such as i) improving the stiffness and strength of recycled carbon fibers by optimizing the pyrolysis treatment [29], and ii) reducing the energy consumption in the process of curing. This could be achieved, for example, by using the recently emerged volumetric curing processes such as induction heating, microwave heating, or direct electric heating over oven curing [30]. It has been shown that the induction-cured thermoset composites exhibit mechanical properties such as elastic modulus, ultimate tensile strength, and strain-to-failure on par with the oven-cured composites, although the amount of porosity in the induction-cured composites was much higher than in the oven-cured composites [31].

2. MAIN RESULTS OF THE THESIS

2.1. Micro-damage evolution in cross-ply laminates with high crack density

The 90-layers in cross-ply laminates undergo transverse cracking under uniaxial tensile loading. The transverse cracks generate stress perturbations around them, which can be characterized using analytical models available in the literature [7]–[10], [17]. Regarding the distribution of transverse stress in the damaged 90-layers, these models either assume a uniform stress state along the ply thickness direction, or they use simple shape functions to model the stress distribution.

In regions with high crack density, the stress perturbations from transverse cracks begin to interact. Thus, a non-uniform stress state is generated along the ply thickness direction, which can only be characterized using semi-analytical models [32]–[35] or using FEM. The FEM numerical analysis in **Paper I** shows significant gradients in the transverse stress along the 90-ply thickness direction for glass-fiber epoxy (GF/EP) and carbon-fiber/epoxy (CF/EP) cross-ply laminates with different values of normalized crack densities (ρ_n), see Fig. 2.1. Note that the transverse crack density, ρ, is normalized with respect to the 90-layer thickness, $2 \times d$, such that $\rho_n = \rho \times 2 \times d$. It can be seen that the stress gradients increase with transverse crack density. These gradients in transverse stress strongly affect the available ERR for the growth of a new transverse crack, see Fig. 2.2. At very high crack density ($\rho_n = 2.0$), compressive stresses are generated near the laminate midplane (see Fig. 2.1), which reduce to zero the ERR available for the growth of a new transverse crack (see Fig. 2.2), completely stopping transverse crack growth.

The ERR for the growth of a new transverse crack is also reduced due to the local delaminations initiated at the tips of the existing transverse cracks. Such local delaminations are caused by high normal and shear stresses at the transverse crack tips. The growth of local delaminations can be studied using compliance-based analytical models, which assume self-similar growth characteristics independent of the delamination length [20], [36]. But FEM numerical analysis in **Paper II** shows that the ERR available for the growth of local delaminations in cross-ply laminates strongly depends on delamination length and transverse crack density, as shown in Fig. 2.3.

A detailed parametric analysis given in **Paper II** concludes that, along with delamination length and transverse crack density, the ERR available for the growth of a local delamination in [0,90]s cross-ply laminates depends on the layer thickness ratio, t_0/t_{90}, and some specific ratios of elastic constants: E_L^0/E_T^{90} and G_{LT}^0/E_T^{90}. For small delaminations, an increase in these ratios reduces the ERR available for delamination growth, whereas for long delaminations, the effect is opposite.

Depending on the local stress state and local variations in fracture toughness, local delaminations can grow into various shapes such as I-shape, T-shape, S-shape, and C-shape. The ERR available for delamination growth also depends on the delamination shape, as shown in Fig. 2.4. The ERR analysis in **Paper II** also shows that non-symmetrical I-shaped delaminations tend to grow into symmetrical delaminations before growing further.

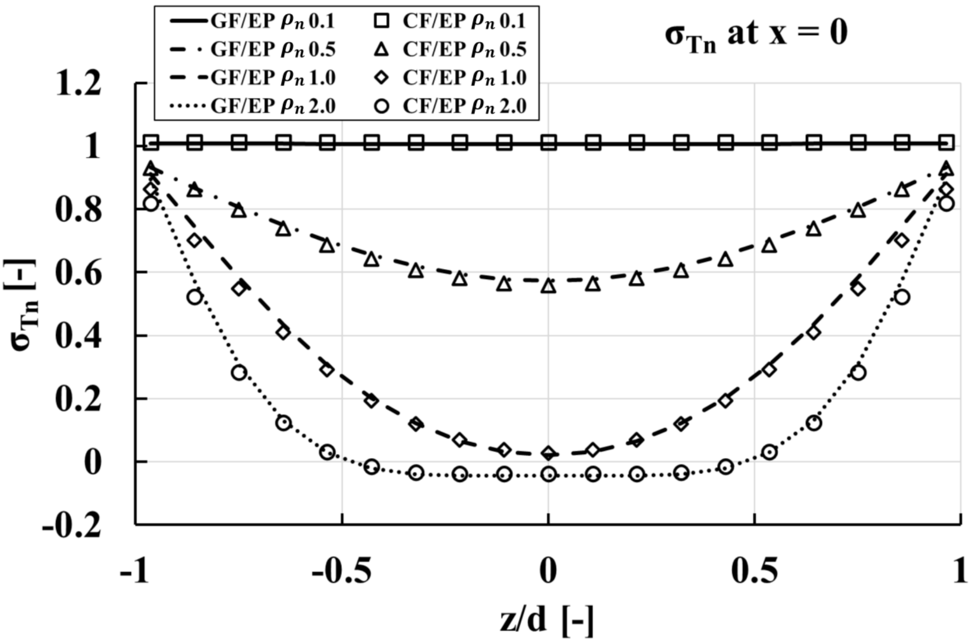

Fig. 2.1. Distribution of normalized transverse stress (σ_{Tn}) in the damaged 90-layer in GF/EP and CF/EP [0,90]s cross-ply laminates along the ply thickness (z-axis) direction. Stress values are normalized with respect to the transverse stress in the undamaged 90-layer. d is half-thickness of the 90-layer. Transverse crack density (ρ) is normalized with respect to $2 \times d$. (Reprinted from **Paper I)**.

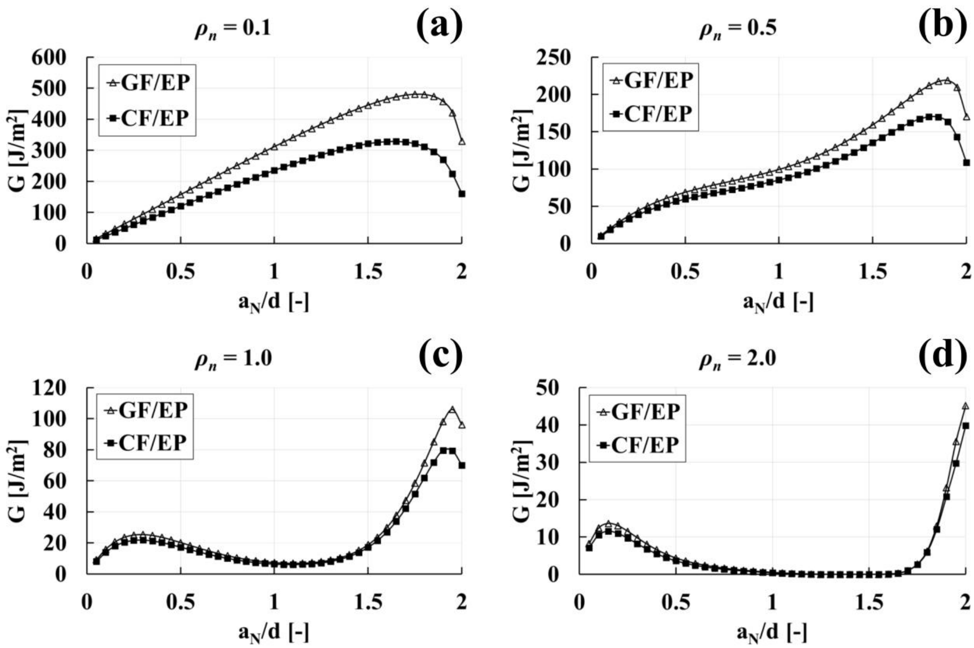

Fig. 2.2. Trends in available energy release rate for the growth of a new transverse crack in the 90-layer in GF/EP and CF/EP [0,90]s cross-ply laminates with normalized crack density: (a) 0.1, (b) 0.5, (c) 1.0, and (d) 2.0. a_N is the transverse crack length. (Reprinted from **Paper I)**.

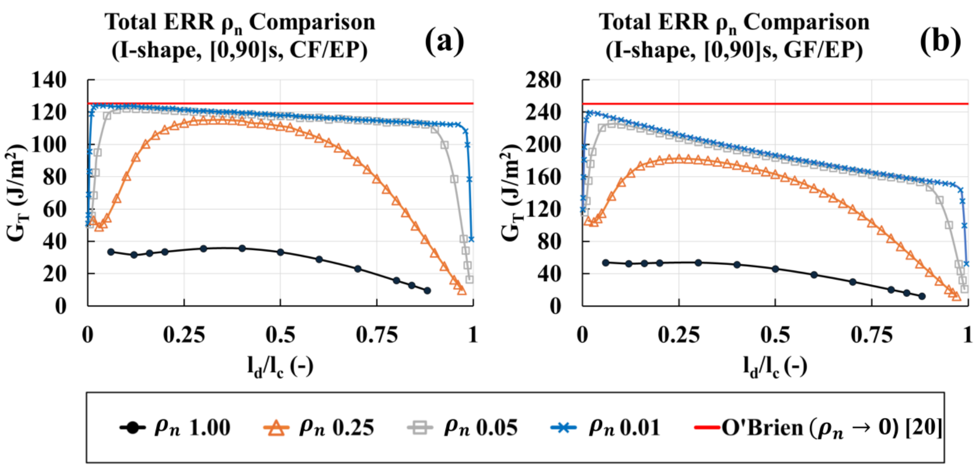

Fig. 2.3. Trends in total available energy release rate for the growth of a local delamination in (a) CF/EP and (b) GF/EP [0,90]s cross-ply laminates for normalized crack densities 1.00, 0.25, 0.05, and 0.01 calculated using FEM. The FEM ERR trends are compared with the constant ERR value given by the compliance-based analytical model by O’Brien [20]. (Reprinted from **Paper II)**.

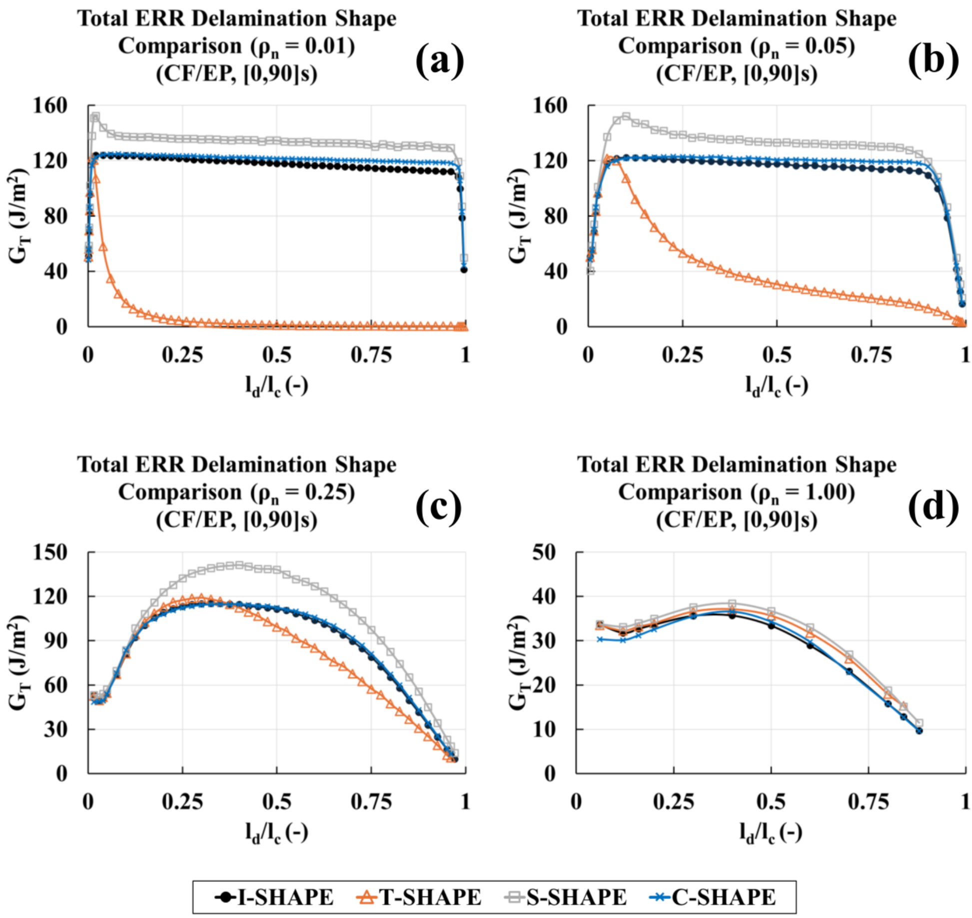

Fig. 2.4. Trends in total available energy release rate for the growth of a local delamination with I-shape, T-shape, S-shape, and C-shape for normalized crack densities: (a) 0.01, (b) 0.05, (c) 0.25, and (d) 1.00. (Reprinted from **Paper II)**.

2.2. Micro-damage evolution in hybrid carbon/steel fiber textile composites

The technique of hybridization with ductile steel fibers has been explored in UD composite laminates to improve mechanical properties (ductility, in particular) and multifunctionality of the composites [37]–[41]. Rehra et al. [38], [39], in their studies on the hybridization of UD carbon-fiber/epoxy laminates with ductile steel fibers, concluded that the relative volume fraction of carbon and steel fibers, and steel fiber/matrix adhesion were important factors that determined the increase in ductility due to hybridization. McBride and O’Brien [40], [41] reported a significant improvement in toughness of hybrid glass/steel fiber UD composites under quasi-static tensile and cyclic loading. Nevertheless, hybridization with ductile steel fibers in composites with a textile meso-structure has not been explored in the literature to date. Thus, **Papers III, IV,** and **V** present the techniques of manufacturing, mechanical testing, and micro-damage analysis of composites with hybrid carbon/steel fiber textile reinforcement.

Table 2.1

Hybrid and Non-Hybrid Textile Composite Configurations

Type		Notation	Lay-up
Knitted	Reference non-hybrid	C1	$[(T300)_8]$*
		M1	$[(SY\ 11/1)_8]$*
		M2	$[(SY\ 11/1\ 3filaments)_8]$
	Hybrid	H1	$[(Hybrid\ SY11/1{+}T300)_8]$
		H2	$[(T300/SY11/1)]_{2s}$
Woven	Reference non-hybrid	C4	$[T300\ 1x]_4$
		M4	$[SY\ 11/1\ 2x]_3$
	Hybrid	H5	$[T300\ 1x + SY\ 11/1\ 2x]_4^{\#}$
		H6	$[SY\ 11/1\ 2x + T300\ 1x]_4$
		H8	$[(SY\ 11/1\ 2x + T300\ 1x)(T300\ 1x + SY\ 11/1\ 2x)]_{2.5}$
		H9	$[T300\ 1x\ /\ SY\ 11/1\ 2x]_{2.5}$

*T300 – carbon-fiber yarn, SY 11/1 is steel-fiber yarn.

[#] Warp yarn + weft yarn.

Hybrid carbon/steel fiber composites with plain woven and plain weft knitted meso-structures were manufactured using the vacuum infusion method [42]. Composite specimens with hybrid and non-hybrid configurations (as shown in Table 2.1) were tested under uniaxial quasi-static tensile loading along the warp-yarn direction at a 2 mm/min, i.e., 1 %/min displacement rate. A comparison of initial elastic modulus values of the composite specimens is given in Fig. 2.5. It was found that the yarn-level hybridization (refer to configuration H1) yielded composites with higher longitudinal stiffness than the layer-level hybridization (refer to configuration H2) in the case of knitted meso-structure. For woven composites, the longitudinal stiffness values were mainly governed by the yarns along the warp direction.

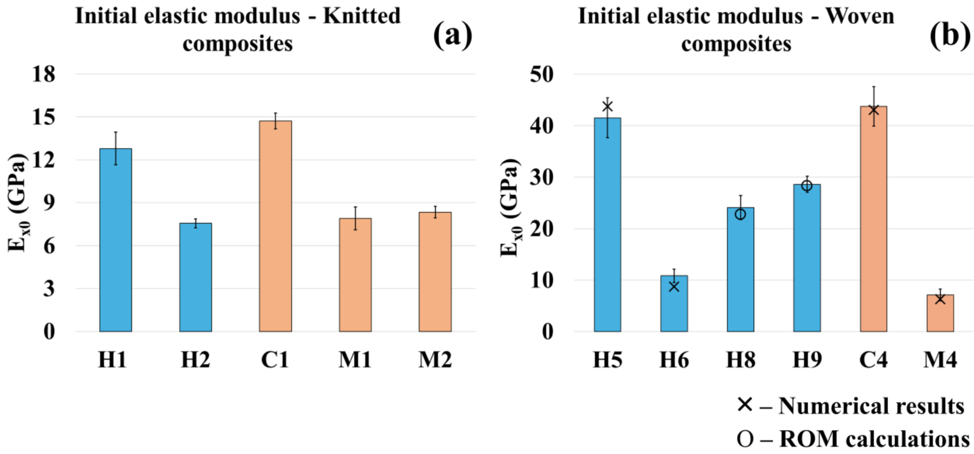

Fig. 2.5. Comparison of initial longitudinal elastic modulus (E_{x0}) values in knitted and woven composite configurations. The cross-marks indicate FEM numerical results. The modulus values for H8 and H9 are calculated using the rule of mixtures (ROM) based on the numerical results for H5, H6, C4 and M4. (Adapted from **Papers III** and **V**).

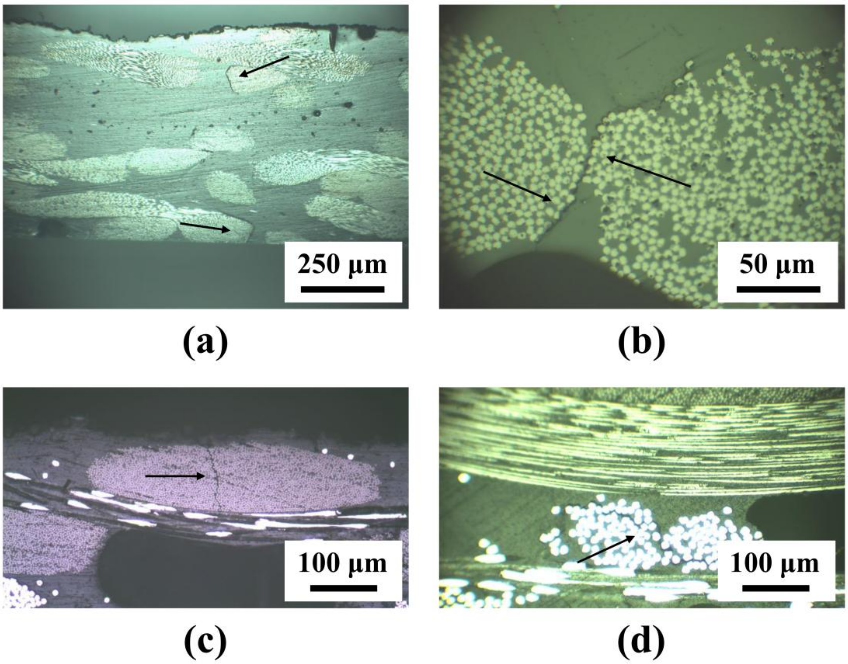

Fig. 2.6. Damage initiation in knitted and woven composites under uniaxial quasi-static tensile loading along the warp yarn direction: (a) yarn/matrix-interface delaminations in C1 at 0.6 % applied strain; (b) carbon-fiber weft-yarn/matrix delamination in H8 at 0.8 % applied strain; (c) transverse crack through carbon-fiber weft-yarn in H8 at 0.8 % applied strain; and (d) shear matrix crack through steel-fiber weft-yarn in H9 at 0.8 % applied strain.

At the applied strain value of 0.6 %, micro-damage initiation was observed in knitted composites along the yarn/matrix interfaces (see Fig. 2.6 (a)). In knitted hybrid composites, the interface delaminations were present only along the carbon fiber yarn/matrix boundaries, and not along the steel fiber yarn/matrix boundaries. In the case of woven composites, micro-damage initiated around the applied strain values of 0.6–0.8 % in the form of carbon fiber weft yarn/matrix delaminations and transverse cracks through carbon fiber weft yarns (see Fig. 2.6 (b), (c)). Shear matrix cracks through steel fiber weft yarns were also observed (see Fig. 2.6 (d)). The damage evolution took place in the form of interconnection of yarn/matrix-interface delaminations in knitted composites and coalescence of transverse cracks and yarn/matrix-interface delaminations in woven composites (see Fig. 2.7).

Comparing the final failure behavior of different composite configurations, the trend in tensile strength values was similar to the longitudinal stiffness values. The knitted composites with yarn-level hybridization exhibited higher longitudinal tensile strength than those with layer-level hybridization. In the case of woven composites, the longitudinal tensile strength was mainly governed by the yarns along the warp direction. The SEM analysis of fracture surfaces of the woven composite specimens showed large longitudinal debonds along the carbon fiber warp yarn/matrix-interface. In woven composite specimens with steel fiber warp yarns, small debonds were observed at the warp yarn/matrix interface, with microscale necking in the steel fibers prior to failure.

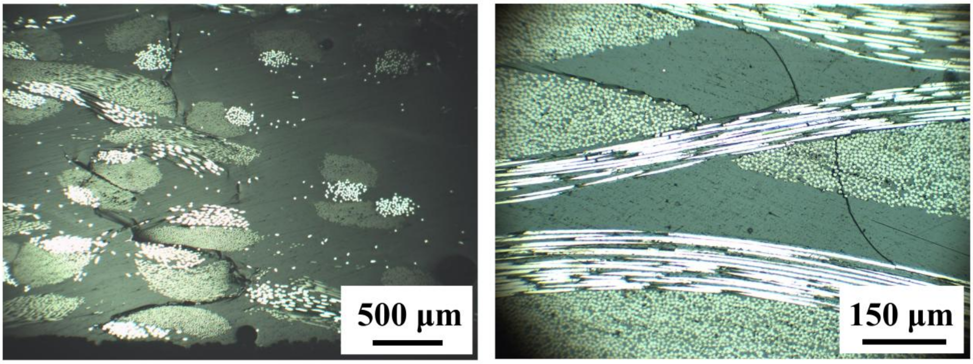

(a) (b)

Fig. 2.7. Damage evolution in knitted and woven composites under uniaxial quasi-static tensile loading along the warp yarn direction: (a) interconnection of yarn/matrix-delaminations in H1 at 1.2 % applied strain; and (b) coalescence of delaminations and transverse cracks in C4 at 0.8 % applied strain. (Adapted from **Paper III**).

The mechanical behavior of hybrid and non-hybrid textile composites was studied numerically using FEM in **Papers IV** and **V**. 3D representative volume elements (RVEs) were generated for the composite configurations H5, H6, C4, and M4. The resin-impregnated fiber yarns were treated as homogeneous composite materials, and their orthotropic material properties were calculated using a micromechanics-based concentric cylinder assembly model.

The yarns had an elliptical cross-section. The warp yarns had sinewave curvature, whereas the weft yarns were assumed straight. The yarns were embedded in a cuboidal matrix block with isotropic material properties. The geometrical specifications of the yarns and the matrix block were determined from optical microscopy images of the composite specimens. The RVEs were further calibrated by comparing their elastic behavior with the experimental data. The assembly of yarns and matrix block was meshed with 3D solid elements in ABAQUS software. To study their behavior under quasi-static tensile loading, the elastoplastic damage model for fiber-reinforced composite materials developed by Cózar et al. [1], [2] was applied to the textile yarns, and the concrete damaged plasticity model [43] available in ABAQUS software was applied to the matrix block.

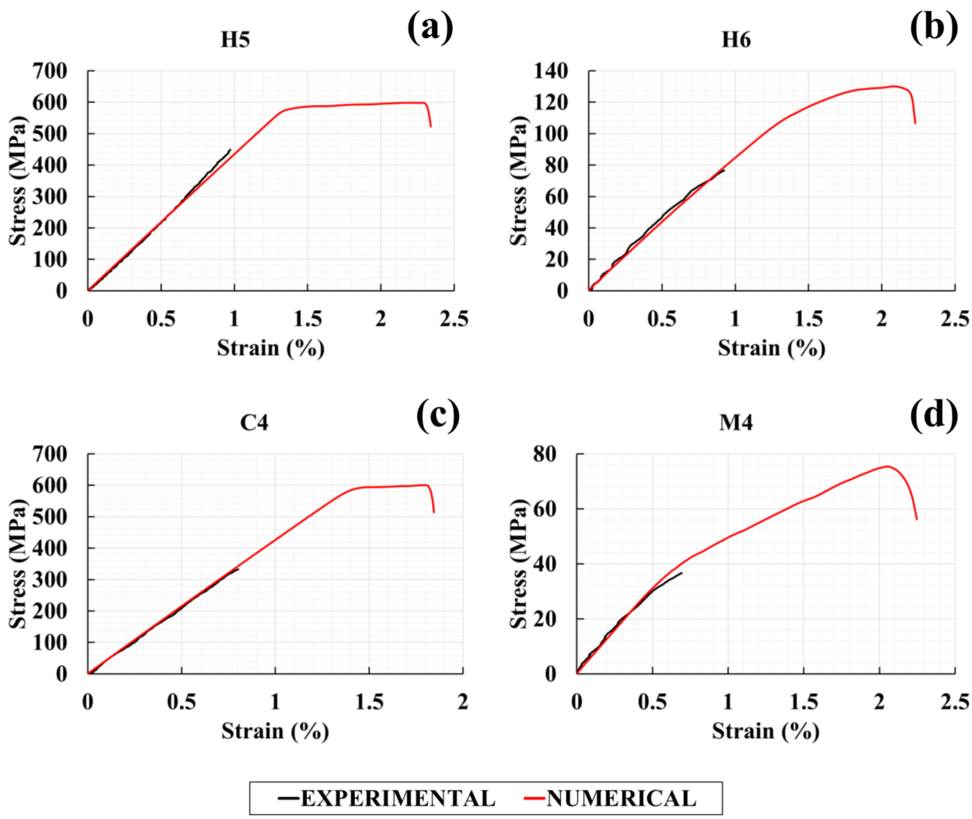

Fig. 2.8. Comparison of the full stress-strain behavior under uniaxial quasi-static tensile loading along the warp yarn direction calculated using experimental and numerical techniques for the composite configurations (a) H5, (b) H6, (c) C4, and (d) M4. (Adapted from **Paper V**).

A comparison of the full stress-strain behavior of the composite configurations calculated using experimental and numerical techniques is given in Fig. 2.8. The experimental stress-strain curves match closely with the numerical curves in the linear elastic stage. As shown in Fig. 2.8, the numerical curves provide further insight into the non-linear plastic and damage evolution behavior of the composite configurations. In the hybrid configuration H5, the numerical stress-strain curve shows linear elastic behavior until micro-damage initiates in the form of matrix cracking at the weft yarn/matrix interface at 1.2 % applied strain. This damage event at the steel fiber weft yarns does not change the slope of the stress-strain curve, as the macro-mechanical behavior of H5 is mainly governed by the carbon fiber warp yarns. As can be seen in Fig. 2.9, a knee point is observed in the stress-strain curve at 1.37 % applied strain, which is caused by the initiation of fiber failure (denoted by damage parameter D_L) in the warp yarn. Along the plateau region seen in the stress-strain curve, the fiber damage distributes across the warp yarn, creating multiple clusters of fiber damage shown in red color in the damage contour plots. Finally, at an applied strain of 2.3 %, the warp yarn fails at one of the fiber damage clusters, and the composite undergoes ultimate failure.

Paper V presents a parametric analysis of the full stress-strain behavior of the hybrid composite configuration H5, calculated using FEM. As the behavior of a textile composite under tensile loading along the warp yarn direction is mainly governed by the warp yarn characteristics, the warp yarn strength properties X_T (longitudinal tensile strength), Y_T (transverse tensile strength), and S_L (longitudinal shear strength) were chosen for the parametric analysis. As shown in Fig. 2.10 (a), it was observed that X_T affects the knee point in the stress-strain curve, i.e., the initiation of fiber damage in the warp yarn. A lower value of Y_T, as shown in Fig. 2.10 (b), results in a reduction in the ultimate tensile strength due to changes in overall damage evolution characteristics. Finally, the change in S_L, see Fig. 2.10 (c), causes a change in the distribution of damage in the warp yarn after the initiation of fiber damage, slightly altering the strain-to-failure.

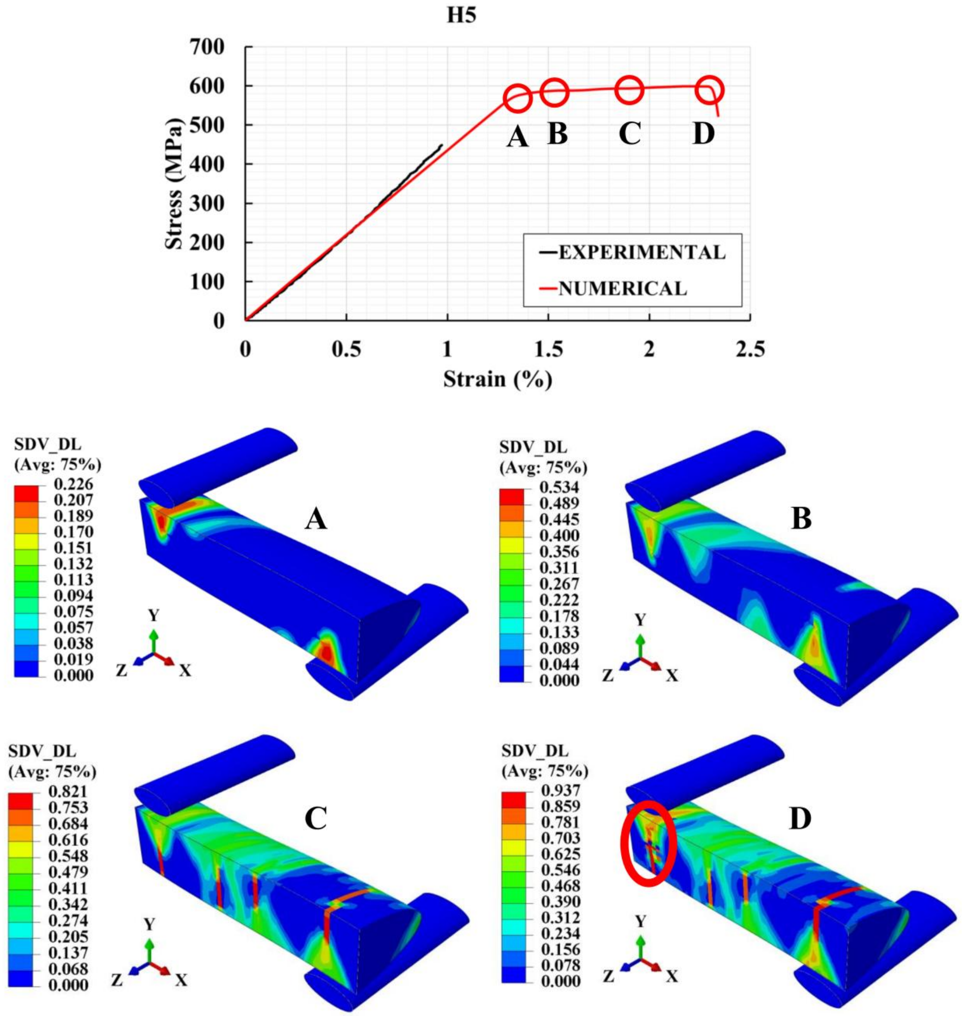

Fig. 2.9. Evolution of longitudinal damage (D_L), i.e., fiber breakage, in the warp yarn of the hybrid composite configuration H5 under quasi-static tensile loading along the warp yarn direction. (Adapted from **Paper V**).

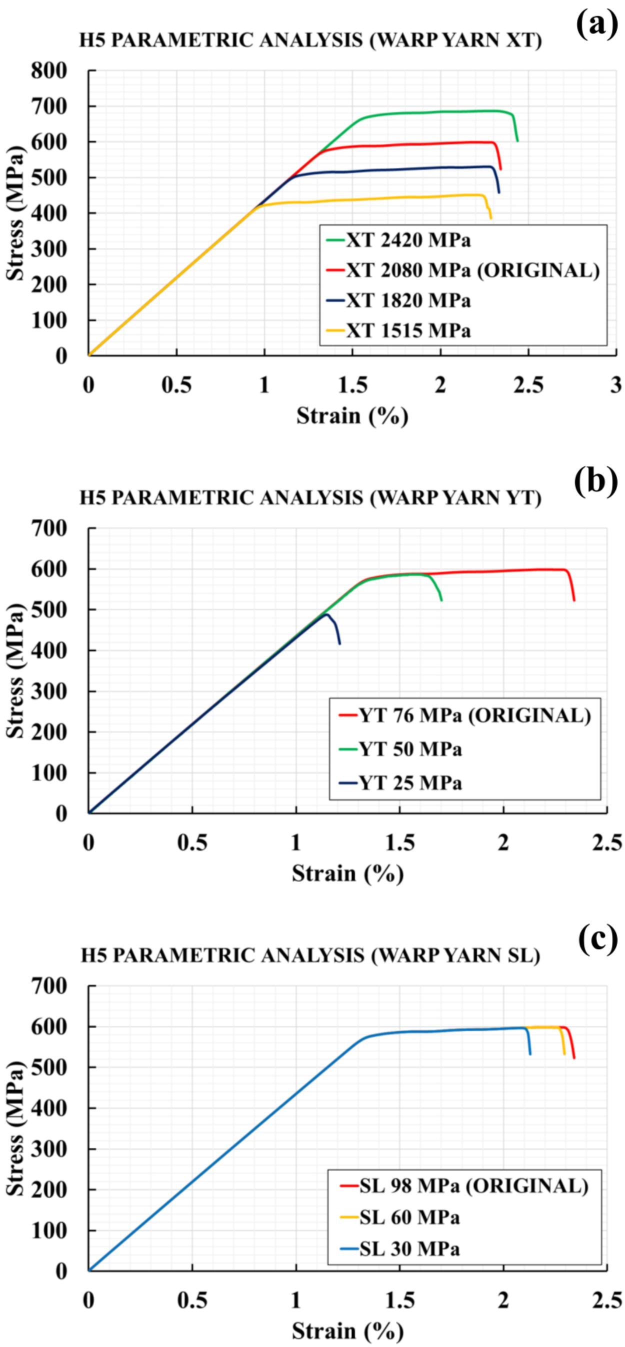

Fig. 2.10. Parametric analysis of the full stress-strain behavior of the hybrid composite configuration H5 under uniaxial tensile loading along the warp yarn direction, by varying (a) warp yarn longitudinal strength X_T; (b) warp yarn transverse strength Y_T; and (c) warp yarn longitudinal shear strength S_L. (Reprinted from **Paper V**).

2.3. Micro-damage evolution in induction-cured thermoset composites

Despite their excellent mechanical properties, the use of carbon-fiber-reinforced thermoset composites is limited to high-value engineering sectors due to the high cost of raw materials and manufacturing. The costs in manufacturing can be reduced by choosing a less energy-intensive alternative to the conventional autoclave method for the curing of thermoset resin [30]. Volumetric heating methods, such as microwave heating and electromagnetic induction heating, can be such energy-efficient alternatives for thermoset curing, where heat is generated from inside the composite part [44], [45].

Induction heating of carbon-fiber-reinforced thermoset composites requires a closed loop of carbon fiber reinforcement, which can be achieved using multi-layered composite laminates with meso-structures such as textile and cross-ply [46], [47]. An induction coil supplied with an alternating current induces current inside the closed-loop of carbon fibers with the help of an oscillating magnetic field, and the carbon fiber reinforcement gets heated due to different mechanisms, such as Joule losses, dielectric hysteresis, and contact resistance heating [48]–[50]. This, in turn, heats the thermoset matrix around the current-carrying carbon fibers, which can ultimately lead to the curing of the thermoset resin.

Induction heating of CF-reinforced thermoset composites is very sensitive to the distance between the induction coil and the workpiece (here, the composite part), as the maximum temperature reached in the workpiece has an inverse-square relation with the distance from the induction coil [51]. Also, it has been observed that the heating pattern on a textile or cross-ply composite resembles the coil shape [52]. In the case of a commonly used circular induction coil, it would make a near-circular heating pattern on the composite workpiece, creating a cold spot in the middle [53]. The generation of cold spots in the composite workpiece prevents uniform curing of the thermoset resin.

Using a novel moving-coil induction-heating setup described in **Paper VI**, a near-uniform cure of the epoxy resin in CF-reinforced [0,90]s cross-ply composites was attempted. According to the recommended curing cycles for the material system used in the present study, i.e., XC130-C12UD-300(300) high-strength UD carbon fiber epoxy prepreg [54], the curing cycle of 4 hours at 100 °C was chosen based on the capabilities of the induction heating system. Uniformity of curing was assessed using a degree-of-cure analysis by differential scanning calorimetry (DSC) during the pilot test. Figure 2.11 shows the glass transition temperature (T_g) values for induction-cured and oven-cured composite reference specimens that is directly proportional to the degree of cure. A significant variation, up to 20 %, is observed in the T_g values of induction-cured composite specimens, with the average value of glass transition temperature lower in the induction-cured than in the oven-cured composite specimens.

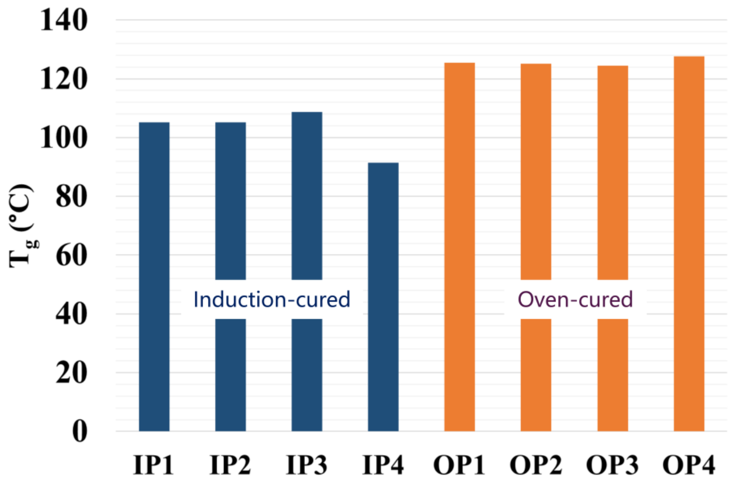

Fig. 2.11. Glass transition temperature (T_g) values in induction-cured (IP1–IP4) and oven-cured (OP1–OP4) specimens indicating the degree of cure. (Adapted from **Paper VI**).

Following the pilot test, the predetermined path for the induction coil movement was improved to manufacture a new 300 mm × 300 mm composite plate with a [0,90]s cross-ply layup using induction heating. Rectangular specimens were cut from different locations on the cured composite plate, and the variation in mechanical properties at these locations was studied using quasi-static tensile testing. Analysis of the mechanical properties of the new induction-cured composite specimens is currently ongoing.

In Fig. 2.12 and Table 2.2 it can be seen that although the mechanical properties varied considerably, up to 9 %, across different locations on the induction-cured composite plate, the average values of elastic modulus, ultimate tensile strength, and strain-to-failure of the induction-cured specimens are still within 6 % difference as compared to the oven-cured reference specimens.

Induction heating using a moving-coil setup generates a transient temperature gradient in the workpiece. This forms soft and hard regions in a composite plate cured using the moving-coil setup. The air trapped inside the laminate can escape easily through the soft regions, but not through the hard regions. As the soft regions are always surrounded by the cold, hard regions, air remains trapped during the moving-coil induction curing process. Thus, it was observed that the induction-cured composite plates had a large number of voids. These voids served as the micro-damage initiation sites in the composite specimens. Figure 2.13 shows a transverse crack in an induction-cured composite specimen initiated near a large void. Due to the high void content, all induction-cured composite specimens showed damage initiation and evolution at lower applied strain levels than the oven-cured reference specimens, as shown in Fig. 2.14.

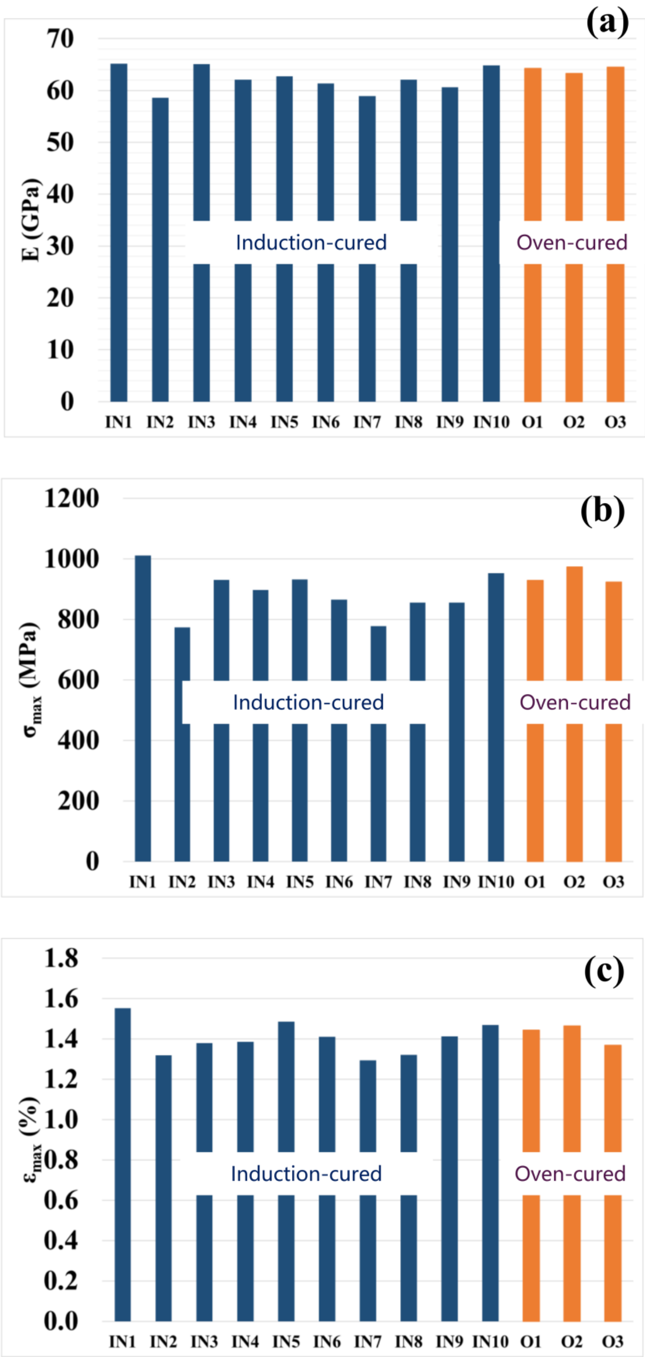

Fig. 2.12. Comparison of (a) longitudinal elastic modulus, (b) ultimate tensile strength, and (c) strain-to-failure values in induction-cured and oven-cured [0,90]s cross-ply laminates under uniaxial quasi-static tensile loading.

Table 2.2

Comparison of Average Mechanical Properties of Induction-Cured and Oven-Cured Composite Specimens

	Induction-cured	Oven-cured	Difference in %
Elastic modulus (GPa)	62.14 ± 2.40	64.04 ± 0.64	2.95
Tensile strength (MPa)	885.53 ± 75.37	941.96 ± 27.54	5.99
Strain-to-failure (%)	1.40 ± 0.08	1.43 ± 0.05	1.58

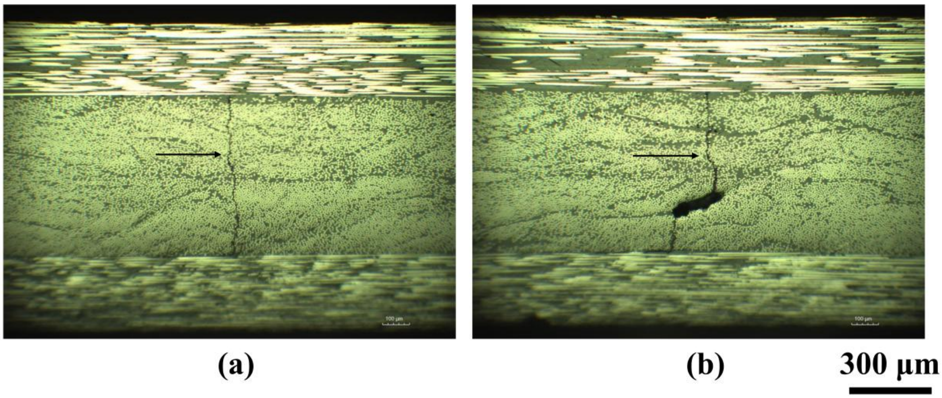

Fig. 2.13. Transverse cracks generated in induction-cured [0,90]s cross-ply composite specimens under uniaxial quasi-static tensile loading: (a) at a random location in the 90-layer, and (b) near a large void.

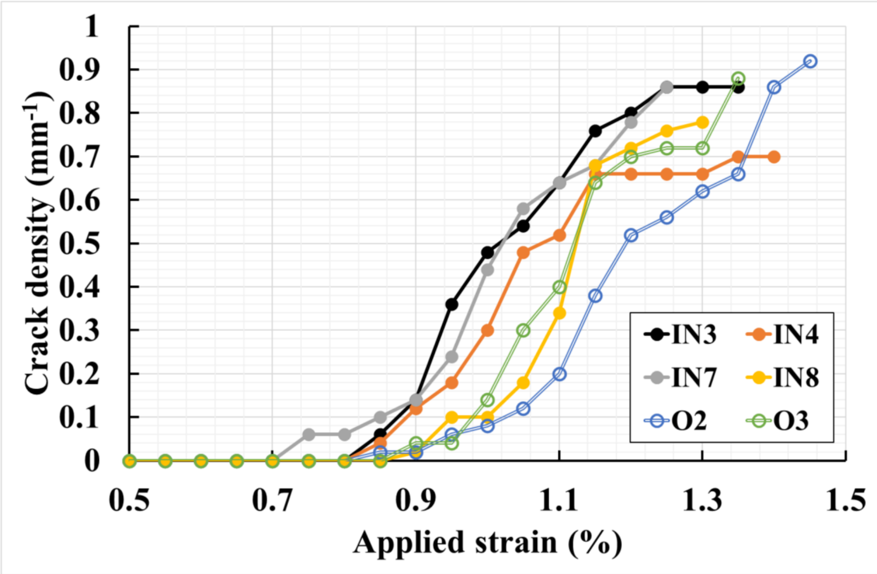

(a)

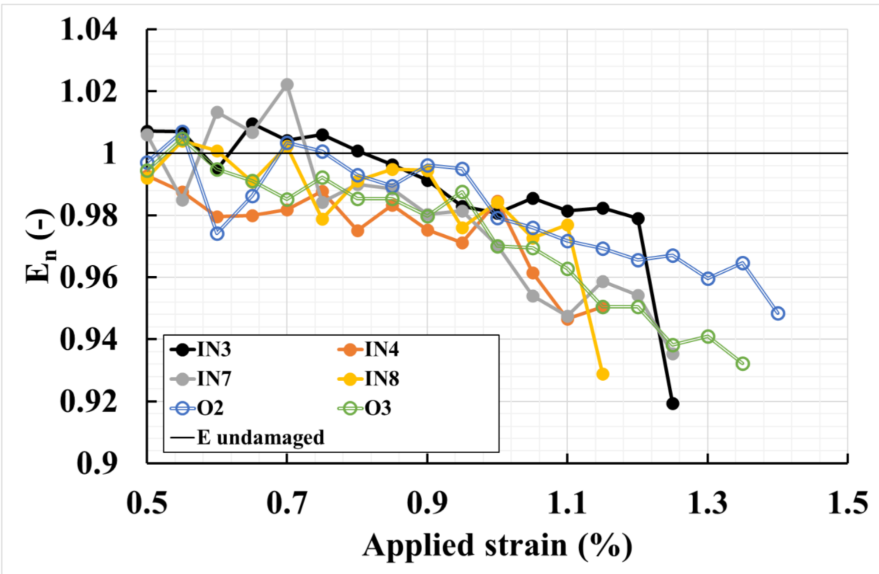

(b)

Fig. 2.14. (a) Evolution of transverse crack density in induction-cured and oven-cured [0,90]s cross-ply laminates with increasing applied strain level, and (b) corresponding reduction in the longitudinal stiffness value of the composite specimens.

3. CONCLUSIONS

In the Thesis, micro-damage evolution was studied in (a) cross-ply laminates with high crack density, (b) hybrid carbon/steel fiber textile composites, and (c) induction-cured thermoset composites. The main conclusions of the study are as follows

1. High transverse stress gradients are created in the regions with high crack density in 90-layer in cross-ply laminates under uniaxial tensile loading. The stress gradients strongly affect the strain energy release rate available for the growth of a new transverse crack. In the regions with ultra-high crack density (crack density multiplied by 90-layer thickness > 2.0), the compressive stresses generated near the laminate midplane due to high stress gradients completely stop the growth of a new transverse crack.
2. At the tips of the existing transverse cracks in cross-ply laminates under uniaxial tensile loading, the generation of local delaminations takes place due to high stress concentration. The local delamination growth is strongly affected by the transverse crack density, 0/90-layer thickness ratio, and the specific ratios of elastic moduli of 0- and 90-layers, such as E_L^0/E_T^{90} and G_{LT}^0/E_T^{90}. The non-symmetrical I-shaped delaminations tend to grow into symmetrical I-shaped delaminations before growing further.
3. Damage initiation takes place in the form of weft yarn/matrix-interface delaminations in hybrid carbon/steel fiber woven composites under uniaxial tensile loading along the warp yarn direction. This damage event at the weft yarns does not affect the slope of the stress-strain curve of a hybrid composite with carbon fiber warp yarns, as in this case, the composite's macro-mechanical behavior is mainly governed by the warp yarn properties.
4. A knee point is observed in the stress-strain curve of a hybrid carbon/steel fiber woven composite with carbon fiber warp yarns when fiber damage is initiated in the warp yarns. Upon further loading, damage evolution takes place with the distribution of fiber damage and the formation of multiple clusters of fiber breaks. The failure of warp yarn takes place at a fiber-break cluster, which in turn results in the ultimate failure of the hybrid composite.
5. In the composites manufactured using a moving-coil induction heating setup, large void formation due to entrapment of air bubbles results in the initiation and evolution of micro-damage at a lower applied strain level than in the oven-cured composites.

BIBLIOGRAPHY

[1] Cózar IR, Otero F, Maimí P, González E V., Miot S, Turon A, et al. A three-dimensional plastic-damage model for polymer composite materials. Compos Part A Appl Sci Manuf 2022; 163. https://doi.org/10.1016/j.compositesa.2022.107198.

[2] Cózar IR, Otero F, Maimí P, González E V., Turon A, Camanho PP. An enhanced constitutive model to predict plastic deformation and multiple failure mechanisms in fibre-reinforced polymer composite materials. Compos Struct 2024; 330. https://doi.org/10.1016/j.compstruct.2023.117696.

[3] París F, Correa E, Mantič V. Kinking of transversal interface cracks between fiber and matrix. Journal of Applied Mechanics, Transactions ASME 2007;74. https://doi.org/10.1115/1.2711220.

[4] Gorbatikh L, Lomov S V. Damage accumulation in textile composites. Modeling Damage, Fatigue and Failure of Composite Materials, 2016. https://doi.org/10.1016/B978-1-78242-286-0.00003-0.

[5] Nairn JA. Matrix Microcracking in Composites. Comprehensive Composite Materials, 2000. https://doi.org/10.1016/b0-08-042993-9/00069-3.

[6] Blázquez A, Mantič V, París F, McCartney LN. Stress state characterization of delamination cracks in [0/90] symmetric laminates by BEM. Int J Solids Struct 2008; 45: 1632–62. https://doi.org/10.1016/J.IJSOLSTR.2007.10.013.

[7] Lim SG, Hong CS. Prediction of Transverse Cracking and Stiffness Reduction in Cross-Ply Laminated Composites. J Compos Mater 1989; 23: 695–713. https://doi.org/10.1177/002199838902300704.

[8] Hashin Z. Analysis of cracked laminates: a variational approach. Mechanics of Materials 1985; 4. https://doi.org/10.1016/0167-6636(85)90011-0.

[9] Varna J, Berglund L. Multiple transverse cracking and stiffness reduction in cross-ply laminates. Journal of Composites Technology and Research 1991; 13. https://doi.org/10.1520/ctr10213j.

[10] Varna J, Berglund LA. Thermo-elastic properties of composite laminates with transverse cracks. Journal of Composites Technology and Research 1994; 16. https://doi.org/10.1520/ctr10397j.

[11] Berthelot JM. Transverse cracking and delamination in cross-ply glass-fiber and carbon-fiber reinforced plastic laminates: Static and fatigue loading. Appl Mech Rev 2003; 56. https://doi.org/10.1115/1.1519557.

[12] Lomov S V., Ivanov DS, Truong TC, Verpoest I, Baudry F, Vanden Bosche K, et al. Experimental methodology of study of damage initiation and development in textile composites in uniaxial tensile test. Compos Sci Technol 2008;68. https://doi.org/10.1016/j.compscitech.2007.07.005.

[13] Kulkarni AN, Pupurs A, Šņepsts A, Irbe M. MICRO-DAMAGE EVOLUTION IN HYBRID CARBON/STEEL KNITTED AND WOVEN FABRIC COMPOSITES. In: Falzon B, McCarthy C, editors. Proceedings of the 2023 International Conference on Composite Materials, Belfast: Queen's University Belfast; 2023.

[14] Kulkarni AN, Pupurs A, Kononova O, Jevstigņejevs V, Maimi P, Subramani A. Hybrid carbon/steel fiber textile composites for ductility improvements. n.d.
[15] Chen J, Yu Z, Jin H. Nondestructive testing and evaluation techniques of defects in fiber-reinforced polymer composites: A review. Front Mater 2022;9. https://doi.org/10.3389/fmats.2022.986645.
[16] Kulkarni AN. Energy and Strength-based Criteria for Intralaminar Crack Growth in Regions with High Stress Gradients. Independent thesis Advanced level (degree of Master (Two Years)). Luleå University of Technology, 2021.
[17] Garrett KW, Bailey JE. Multiple transverse fracture in 90° cross-ply laminates of a glass fibre-reinforced polyester. J Mater Sci 1977; 12: 157–68. https://doi.org/10.1007/BF00738481.
[18] Kulkarni AN, Pupurs A, Varna J. Analysis of initiation and growth of new transverse cracks in high crack density regions in cross-ply laminates. J Compos Mater 2025; 59: 539–50. https://doi.org/10.1177/00219983241295811.
[19] Berthelot JM, Le Corre JF. Statistical analysis of the progression of transverse cracking and delamination in cross-ply laminates. Compos Sci Technol 2000; 60: 2659–69. https://doi.org/10.1016/S0266-3538(00)00140-8.
[20] O'Brien TK. ANALYSIS OF LOCAL DELAMINATIONS AND THEIR INFLUENCE ON COMPOSITE LAMINATE BEHAVIOR. ASTM Special Technical Publication, 1985. https://doi.org/10.1520/stp36310s.
[21] Wang ASD, Kishore NN, Li CA. Crack development in graphite-epoxy cross-ply laminates under uniaxial tension. Compos Sci Technol 1985; 24. https://doi.org/10.1016/0266-3538(85)90058-2.
[22] Kim TW, Kim HJ, Im S. Delamination crack originating from transverse cracking in cross-ply composite laminates under extension. Int J Solids Struct 1991; 27: 1925–41. https://doi.org/10.1016/0020-7683(91)90186-J.
[23] Kulkarni AN, Pupurs A, Varna J. Parameters affecting growth of local delaminations at transverse crack tips in [0m,90n]s cross-ply laminates. Eng Fract Mech 2025; 328: 111549. https://doi.org/10.1016/J.ENGFRACMECH.2025.111549.
[24] Wang L, Wu J, Chen C, Zheng C, Li B, Joshi SC, et al. Progressive failure analysis of 2D woven composites at the meso-micro scale. Compos Struct 2017; 178. https://doi.org/10.1016/j.compstruct.2017.07.023.
[25] Callens MG, Gorbatikh L, Verpoest I. Ductile steel fibre composites with brittle and ductile matrices. Compos Part A Appl Sci Manuf 2014; 61: 235–44. https://doi.org/10.1016/J.COMPOSITESA.2014.02.006.
[26] Allaer K, De Baere I, Lava P, Van Paepegem W, Degrieck J. On the in-plane mechanical properties of stainless steel fibre reinforced ductile composites. Compos Sci Technol 2014; 100. https://doi.org/10.1016/j.compscitech.2014.05.009.
[27] Czél G, Wisnom MR. Demonstration of pseudo-ductility in high performance glass/epoxy composites by hybridisation with thin-ply carbon prepreg. Compos Part A Appl Sci Manuf 2013; 52. https://doi.org/10.1016/j.compositesa.2013.04.006.

[28] Swolfs Y, Verpoest I, Gorbatikh L. Recent advances in fibre-hybrid composites: materials selection, opportunities and applications. International Materials Reviews 2019; 64. https://doi.org/10.1080/09506608.2018.1467365.

[29] Corvo Alguacil M, Umeki K, Gaidukovs S, Barkāne A, You S, Joffe R. The impact of thermal treatment parameters on the preservation of carbon fiber mechanical properties after reclamation. Current Research in Green and Sustainable Chemistry 2024; 9. https://doi.org/10.1016/j.crgsc.2024.100431.

[30] Collinson MG, Bower MP, Swait TJ, Atkins CP, Hayes SA, Nuhiji B. Novel composite curing methods for sustainable manufacture: A review. Composites Part C: Open Access 2022; 9. https://doi.org/10.1016/j.jcomc.2022.100293.

[31] Pupurs A, Lācis V, Šņepsts A, Kulkarni AN, Irbe M. ANALYSIS OF MICRO-DAMAGE EVOLUTION IN INDUCTION-CURED THERMOSET COMPOSITES. In: Binetruy C, Jacquemin F, editors. Proceedings of the 21st European Conference on Composite Materials, Nantes: The European Society for Composite Materials (ESCM) and the Ecole Centrale de Nantes; 2024, pp. 1529–34.

[32] McCartney LN, Schoeppner GA. Predicting the effect of non-uniform ply cracking on the thermoelastic properties of cross-ply laminates. Compos Sci Technol 2002; 62. https://doi.org/10.1016/S0266-3538(02)00091-X.

[33] Hajikazemi M, Sadr MH. A variational model for stress analysis in cracked laminates with arbitrary symmetric lay-up under general in-plane loading. Int J Solids Struct 2014; 51. https://doi.org/10.1016/j.ijsolstr.2013.10.024.

[34] Hajikazemi M, Sadr MH, Hosseini-Toudeshky H, Mohammadi B. Thermo-elastic constants of cracked symmetric laminates: A refined variational approach. Int J Mech Sci 2014; 89. https://doi.org/10.1016/j.ijmecsci.2014.08.008.

[35] Hajikazemi M, McCartney LN. Comparison of Variational and Generalized Plane Strain approaches for matrix cracking in general symmetric laminates. International Journal of Damage Mechanics 2018; 27. https://doi.org/10.1177/1056789516685381.

[36] Rahmani M, Farrokhabadi A. Prediction of induced delamination development in [θ/90]s composite laminates using a computational analytical approach. Compos Struct 2018; 203. https://doi.org/10.1016/j.compstruct.2018.07.018.

[37] Hannemann B, Backe S, Schmeer S, Balle F, Breuer UP. New multifunctional hybrid polymer composites reinforced by carbon and steel fibers. ICCM International Conferences on Composite Materials, vol. 2015, July, 2015.

[38] Rehra J, Hannemann B, Schmeer S, Hausmann J, Breuer UP. Approach for an Analytical Description of the Failure Evolution of Continuous Steel and Carbon Fiber Hybrid Composites. Adv Eng Mater 2019; 21. https://doi.org/10.1002/adem.201800565.

[39] Rehra J, Jungbluth J, Katri B, Schmeer S, Gurka M, Balle F, et al. Damage and failure mechanisms of hybrid carbon fiber and steel fiber reinforced polymer composites. Compos Part A Appl Sci Manuf 2024; 185: 108366. https://doi.org/10.1016/j.compositesa.2024.108366.

[40] McBride AK, Turek SL, Zaghi AE, Burke KA. mechanical behavior of hybrid glass/steel fiber reinforced epoxy composites. Polymers (Basel) 2017; 9. https://doi.org/10.3390/polym9040151.
[41] O'Brien C, Zaghi AE. Mechanical characteristics of hybrid composites with ±45° glass and 0°/90° stainless steel fibers. Materials 2018; 11. https://doi.org/10.3390/ma11081355.
[42] Andrejs P, Inita B, Inga Ļ, Māris M, Mārtiņš I, Alens Š. MANUFACTURING AND EXPERIMENTAL TESTING OF COMPOSITE/METAL JOINTS WITH TEXTILE MESOSTRUCTURE. ECCM 2022 - Proceedings of the 20th European Conference on Composite Materials: Composites Meet Sustainability, vol. 2, 2022.
[43] Concrete Damaged Plasticity. ABAQUS Analysis User's Guide, vol. Volume III Materials, 2016.
[44] Thostenson ET, Chou TW. Microwave and conventional curing of thick-section thermoset composite laminates: Experiment and simulation. Polym Compos 2001; 22: 197–212. https://doi.org/10.1002/PC.10531.
[45] Bayerl T, Duhovic M, Mitschang P, Bhattacharyya D. The heating of polymer composites by electromagnetic induction – A review. Compos Part A Appl Sci Manuf 2014; 57. https://doi.org/10.1016/j.compositesa.2013.10.024.
[46] Becker S, Mitschang P. Influence of thread count of carbon twill textile-reinforced polyamide 66 laminates on the inductive heating behavior. Journal of Thermoplastic Composite Materials 2021; 34. https://doi.org/10.1177/0892705719854493.
[47] Kidangan RT, Unnikrishnakurup S, Krishnamurthy CV, Balasubramaniam K. The influence of interlaminar microstructure on the induction heating patterns of CFRP laminates. Mater Today Commun 2022; 33. https://doi.org/10.1016/j.mtcomm.2022.104338.
[48] Miller AK, Chang C, Payne A, Gur M, Menzel E, Peled A. The nature of induction heating in graphite-fiber, polymer-matrix composite material. SAMPE Journal 1990; 26.
[49] Fink BK, McCullough RL, Gillespie JW. A local theory of heating in cross-ply carbon fiber thermoplastic composites by magnetic induction. Polym Eng Sci 1992; 32. https://doi.org/10.1002/pen.760320509.
[50] Kim H, Yarlagadda S, Gillespie JW, Shevchenko NB, Fink BK. A study on the induction heating of carbon fiber reinforced thermoplastic composites. Advanced Composite Materials 2002; 11. https://doi.org/10.1163/156855102753613309.
[51] Rudolf R, Mitschang P, Neitzel M. Induction heating of continuous carbon-fibre-reinforced thermoplastics. Compos Part A Appl Sci Manuf 2000; 31. https://doi.org/10.1016/S1359-835X(00)00094-4.
[52] Uzzell JPN, Pickard LR, Hamerton I, Ivanov DS. Novel cellular coil design for improved temperature uniformity in inductive heating of carbon fibre composites. Mater Des 2024; 237. https://doi.org/10.1016/j.matdes.2023.112551.
[53] Lundström F, Frogner K, Andersson M. Analysis of the temperature distribution in weave-based CFRP during induction heating using a simplified numerical model with a

cross-ply representation. Compos B Eng 2021; 223. https://doi.org/10.1016/j.compositesb.2021.109153.
[54] XC130 Autoclave Cure Component Prepreg – Technical Datasheet – 10/11/2022. n.d.

Anish Niranjan Kulkarni was born in 1997 in Pune, India. He obtained his Bachelor's (Hons) degree (2019) in Metallurgical and Materials Engineering from the National Institute of Technology, Tiruchirappalli, India. Following his bachelor's studies, he was selected for the prestigious EU Erasmus Mundus scholarship to pursue a Joint European Master's degree in Advanced Materials Science and Engineering. Since 2022, he has been a PhD student and Researcher at the Faculty of Mechanical Engineering, Transport and Aeronautics (from 2022, Faculty of Civil and Mechanical Engineering) at Riga Technical University. During his doctoral studies, he has represented his research group at various international conferences and seminars and has been on exchange visits to Luleå University of Technology (Sweden) and the University of Girona (Spain). He currently works on various research projects related to the mechanics of polymer composite materials, notably hybrid textile composites and induction-cured thermoset composites.